18B.5 SIMULATIONS OF GRAVITY WAVE-TURBULENCE INTERACTIONS IN THE STABLE BOUNDARY-LAYER

Benjamin MacCall*[1], Patrick Haines[1], Wen-Yih Sun[2], and Wu-Ron Hsu[3]
[1] Army Research Laboratory, Battlefield Environment Division
White Sands Missile Range, NM
[2] Purdue University, West Lafayette, IN
[3] National Taiwan University, Taipei, Taiwan

1. INTRODUCTION

The stable boundary-layer (SBL), contrary to its ostensible simplicity, exhibits a complicated time-dependent behavior that involves the interactions of several processes over a relatively wide range of scales, including intermittent turbulence. Turbulence is of central importance, because it efficiently modifies the flow state through mixing. For several years, gravity waves have been thought to play a very important role in the production of SBL turbulence, but an ultimate description remains elusive.

This paper details our current efforts to simulate gravity wave-turbulence interactions using a non-hydrostatic, atmospheric model applied to the microscale. The initial set of simulations described in this paper explores three separate processes. The first is the simulation of shear instability and the formation of Kelvin-Helmholtz (KH) billows and secondary structures related to shear instability. The second process is the generation of longer wavelength modes which are capable of propagating away from the shear layer. These modes are implicated in the transport of momentum and energy far from a shear layer and may be important for generating the kinds of step-like velocity and temperature profiles observed in the SBL. The final process incorporates idealized terrain elements. The enhanced influence of surface heterogeneity in SBLs has been recognized for several years. Recent work opens the possibility of gravity wave interactions with viscous instability in the presence of topography. The viscous instability can radiate gravity waves or a freely propagating gravity wave can excite viscous instability near the surface (Wu and Zhang 2008).

2. MODEL

We employed the National Taiwan University/ Purdue University (NTU/PU) non-hydrostatic model (Hsu and Sun, 2001; Hsu et al., 2000). This model has been previously applied to several different situations, such as lee mountain waves, shallow convection from cold-air outbreaks, simulations of squall-lines, etc. It employs a height-based, terrain-following coordinate for topography and allows grid stretching in all three spatial dimensions. The model also employs a prognostic equation for density in contrast to employing the anelastic assumption and solving the resulting Poisson equation or solving a pressure tendency equation. This solution method also explicitly resolves acoustic waves avoiding the need for time-filtering. To balance the resources required for a small enough time step to satisfy the Courant-Friedrichs-Levvy (CFL) criterion for acoustic waves, we employ two methods to reduce computation. By decreasing the speed of sound, the largest, stable time interval can be increased without affecting the meteorology. In addition, the model uses a split timestep integration scheme to update more slowly varying physics at an appropriate interval. By avoiding the iterative solvers used on Poisson equations, the model is more easily parallelized for efficient use of massively parallel clusters (Hsu and Sun, 2001). The resulting MPI-based code shows just under 90% efficiency when employing 960 processors, not including time spent during output.

The NTU/PU model uses Deardorff's (1980) single-equation eddy-viscosity closure scheme. As part of the preparation for performing high-resolution simulations of the SBL, a Reynolds stress closure scheme has been implemented to include prognostic transport equations for the second-order turbulence correlations (e.g., subgrid momentum flux and heat flux). This scheme is based on the work of Lumley and Zeman (Lumley, 1979; Zeman and Lumley, 1979; Zeman, 1981). The dissipation is formulated using the scheme outlined by Canuto and Minotti (1993) which reduces the dissipation when the subgrid scale (SGS) is not completely within the isotropic, inertial subrange.

3. SHEAR INSTABILITY

Shear instability is the primary source of turbulence production in stable environments. From linear theory, the depth of the shear layer and the stratification determines the band of modes that are amplified– the Kelvin-Helmholtz (KH) modes. Accurately reproducing the growth of these modes can be difficult for atmospheric models because of the stronger diffusion

* Corresponding author address: Benjamin MacCall, Bldg 1622, WSMR, NM 88002; email: ben.maccall@arl.army.mil

and smoothing employed for numerical stability, which tends to slow the growth or eliminate perturbations during the exponential growth phase. Model simulations often use direct numerical simulation (DNS), but DNS is wholly impractical for atmospheric scales.

A series of model runs were performed with a shear layer defined using a hyperbolic tangent and constant Brunt-Väisälä frequency. The stratification used was N=0.02 s^{-1}, which is relatively weak, but reasonable when compared to step-like structures of lesser stratification embedded within the SBL profile (Chimonas 1999). The shear layers were all 100 m thick with a 4.99 m/s velocity difference between the top and bottom, and were centered at 600 m above a no-slip surface. Below the shear layer, the wind velocity was

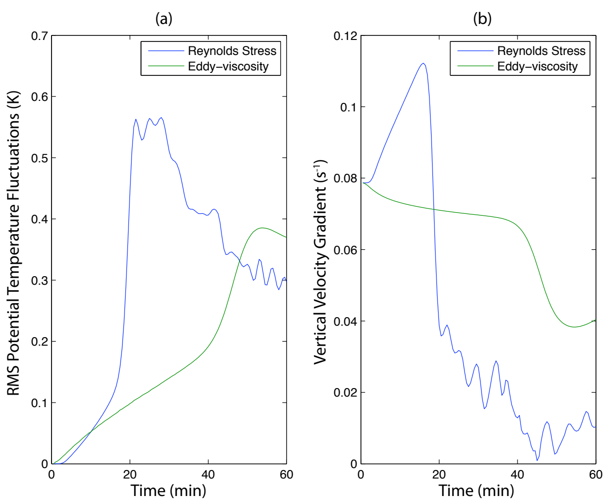

Figure 2: (a) Root mean square potential temperature fluctuations versus time. (b) Mean vertical velocity gradient at the center of the shear layer.

0.01 m/s and 5 m/s above. The minimum gradient Richardson number was Ri=0.06. A 0.0025 m/s perturbation was introduced into the x-velocity field as a single mode, as two modes, or using a pseudo-random number generator. All three simulations produced wave instability and eventual wave breaking (see Fig. 1). Using the eddy-viscosity scheme the diffusion can be reduced, and will produce wave breaking, but with a much slower growth rate. Additionally the model becomes unstable, without significantly increasing the smoothing coefficient. It should be noted that we have not yet experimented with any of the more sophisticated eddy-viscosity closures.

Perturbing with a single 550 m mode, which is within the band of KH modes predicted by linear theory, results in wave fronts perpendicular to the stream-wise direction with no span-wise variation. Fig. 2a compares the fluctuations of the potential temperature between the Reynolds stress model and the single-equation eddy-viscosity model. Again the eddy-viscosity model shows a much slower growth rate. This is echoed in the vertical velocity gradient at the center of the shear layer shown in Fig. 2b. The eroding of velocity shear occurs very quickly once wave breaking occurs for the Reynolds stress model, but even with the wave breaking occurring in the eddy-viscosity model, mixing in the shear layer remains weaker.

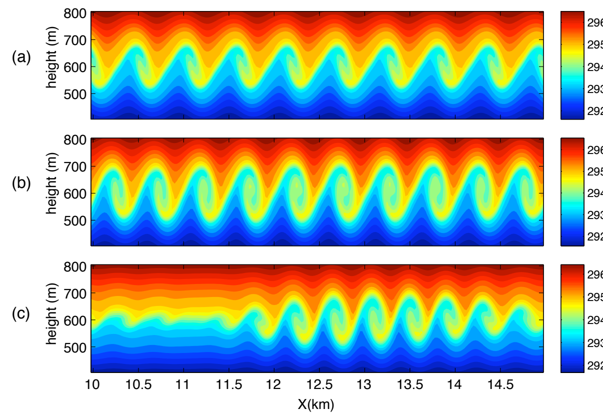

Figure 1: Contours of potential temperature during wave breaking for (a) single mode perturbation, (b) two-mode perturbation, and (c) random perturbation.

When a second unstable KH mode is included, the apparent evolution undergoes some change, but still amplifies a single mode to the point of wave breaking. However, looking at the spectrum of the potential temperature fluctuations (see Fig. 3), we see the excitation of longer wavelength modes. These are gravitational shear waves (e.g. Chimonas and Grant 1984a,b; Fritts 1982, 1984). They have a much longer wavelength than the KH modes and can propagate outside of the shear layer, unlike the KH modes which decay. In addition, they can have a phase speed

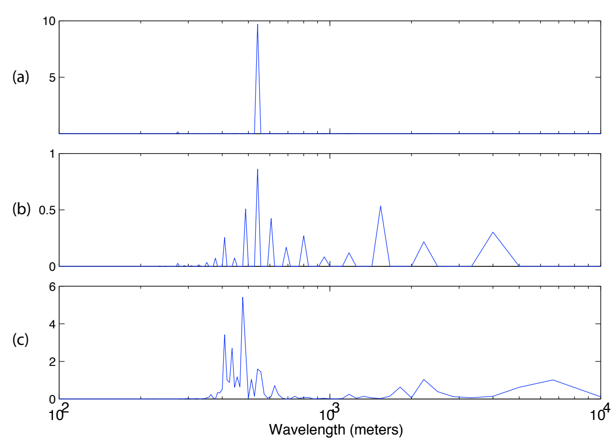

Figure 3: Wave spectrum for fluctuations in the potential temperature after wave breaking for (a) single-mode perturbation (b) two-mode perturbation, and (c) random perturbation.

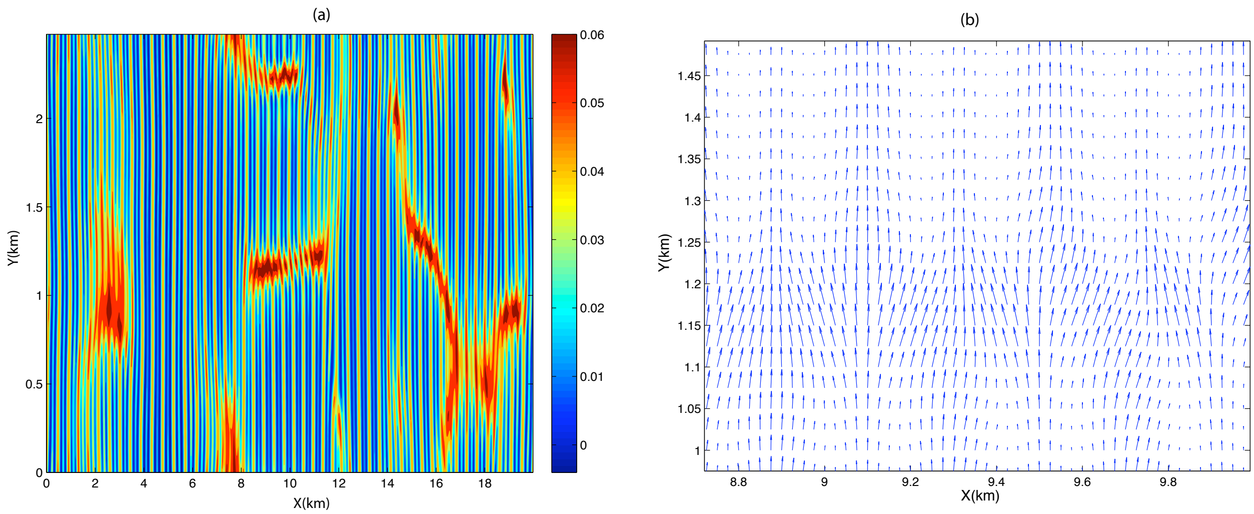

Figure 4: (a) Contours of span-wise vorticity for a slice through the center of the shear layer. (b) Horizontal vorticity vectors for feature in the center of (a). A significant deviation in the direction of the vorticity as stream-wise vorticty is amplified.

different from a velocity within the shear layer. The 5 km waves shown at the left propagate with a phase speed of 5.8 m/s. These waves are generated via nonlinear interactions. While they can be produced by vortex pairing, the stratification outside of the shear layer prevents the pairing. Instead, this effect is likely caused by interactions between the two KH modes introduced during initialization. Again the periodic boundary conditions combined with the span-wise independent perturbation yielded no significant variation in the span-wise direction.

Finally, the same shear layer was perturbed using a pseudo-random number generator. A band of KH modes were excited with a single dominant mode growing to the point of wave breaking. In addition to the growth of several longer wavelength modes as in the two-mode case, span-wise variations were also amplified. These variations correspond with strong deviations in the vorticity vector from the span-wise into both the stream-wise (see Figure 4b) and vertical directions (not shown), and may be related to secondary instability, such as vortex braiding and knotting (Thorpe 1987), which tends to appear early in the instability process. The vorticity perturbations did appear early in these simulations, although they are much smaller than the mean vorticity of the shear layer.

4. TERRAIN SIMULATIONS

Observations point to the increased influence of surface heterogeneity on the flow with effects ranging from drainage currents to shed vortices. Moreover, terrain elements provide an additional source of gravity waves. Recent theoretical work shows the possibility of non-linear interactions between gravity waves and waves resulting from viscous instability near topography (Wu and Zhang 2008). Topography is included through the use of a terrain following coordinate. The two idealized examples we used are the shedding of vortices from an asymmetric, isolated obstacle (Fig. 5a) and the interaction between the flow over a 50 m mountain ridge and an unstable shear layer at 600 m (Fig. 5b). The simulation with the combined shear layer and ridge hint at interesting interactions that enhanced the sub-grid scale turbulent kinetic energy (TKE) between the surface and the shear layer (see Fig 6).

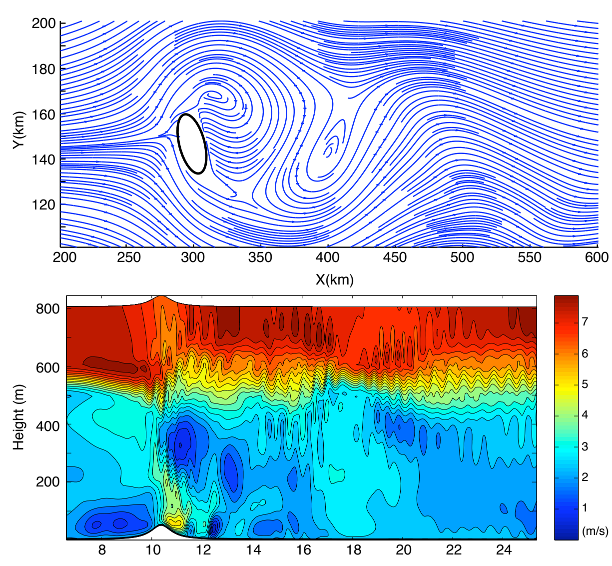

Figure 5: (a) Streamlines of the horizontal flow around a bell-shaped mountain tilted at a 30° angle with respect to the x-axis, and (b) x-velocity contours showing the interaction between flow over a small mountain ridge and a shear layer at 600 m.

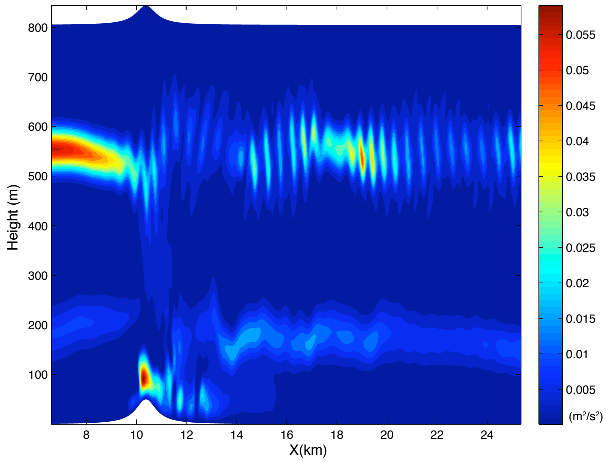

Figure 6: Profile of SGS TKE showing enhancement at a layer between the shear layer at 600 m and the surface.

Being able to directly simulate the generation of these vortices and terrain-produced gravity waves and how they interact with gravitational shear waves, which are also explicitly generated, will allow unprecedented detail. At the same time, these simulations will be able to include the influence of larger scale forcing with a large computational domain. In the near future, we will begin simulations, initialized with data from the CASES-99 experiment, to examine the model's performance for more realistic situations.

ACKNOWLEDGEMENTS

This work was performed while Ben MacCall held a NRC Research Associateship Award at the Army Research Lab White Sands Missile Range. The work is supported by a Department of Defense Challenge Project.

REFERENCES

Canuto, V. M. and Minotti, F. (1993). Stratified turbulence in the atmosphere and oceans: A new subgrid model. Jour. Atmos. Sci., 50(13):1925–1935.

Chimonas, G. (1999). Steps, waves and turbulence in the stably stratified planetary boundary layer. Boundary Layer Meteorology, 90:397–421.

Chimonas, G. and Grant, J. R. (1984a). Shear excitation of gravity waves. part i: Modes of a two-scale atmosphere. J. Atmos. Sci., 41:2269–2277.

Chimonas, G. and Grant, J. R. (1984b). Shear excitation of gravity waves. part ii: Upscale scattering from kelvin-helmholtz waves. J. Atmos. Sci., 41:2278–2288.

Fritts, D. C. (1982). Shear excitation of atmospheric gravity waves. J. Atmos. Sci., 39:1936–1952.

Hsu, W.-R. and Sun, W.-Y. (2001). A time-split, forward-backward numerical model for solving a nonhydrostatic and compressible system of equations. TELLUS, 53A:279–299.

Hsu, W.-R., Sun, W.-Y., Tcheng, S.-C., and Chang, H.-Y. (2000). Parallelization of the ntu-purdue nonhydrostatic numerical model: Simulation of the 11 january 1972 boulder windstorm. The Seventh National Computational Fluid Dynamics Conference.

Lumley, J. L. (1979). Second order modeling of turbulent flows. In Von Karman Institute Lecture Series, number 2. Rhode Saint Genese Belgium.

Mahrt, L. (1999). Stratified atmospheric boundary layers. Boundary-Layer Meteorology, 90:375–396.

Nappo, C. J. and Johansson, P.-E. (1999). Summary of the lovanger international workshop on turbulence and diffusion in the stable planetary boundary layer. Boundary-Layer Meteorology, 90:345–374.

Scinocca, J. F. (1995). The mixing of mass and momentum by kelvin-helmholtz billows. Jour. Atmos. Sci., 52(14):2509–2530.

Wu, X. and Zhang, J. (2008). Instability of a stratified boundary layer and its coupling with internal gravity waves. part 2. coupling with internal gravity waves via topography. J. Fluid Mech., 595:409–433.

Zeman, O. (1981). Progress in the modeling of planetary boundary layers. In Milton Van Dyke, J. V. Wehausen, J. L. L., editor, Annual Review of Fluid Mechanics, volume 13, pages 253–272. Annual Reviews Inc.

Zeman, O. and Lumley, J. L. (1979). Buoyancy effects in entraining turbulent boundary layers: a second-order closure study. In Durst, F., Launder, B., Schmidt, F., and Whitelaw, H., editors, Turbulent Shear Flows I, pages 295–306. Springer-Verlag.